

Nuclear Inst. and Methods in Physics Research, A

Towards a Pixel TPC part I: construction and test of a 32 chip GridPix detector

--Manuscript Draft--

Manuscript Number:	
Article Type:	Full length article
Section/Category:	High Energy and Nuclear Physics Detectors
Keywords:	Micromegas, gaseous pixel detector, micro-pattern gaseous detector, Timepix, GridPix, pixel time projection chamber
Corresponding Author:	Peter Kluit, Ph.D. Nationaal Instituut voor subatomaire fysica Amsterdam, Noord-Holland NETHERLANDS
First Author:	Peter Kluit, Ph.D.
Order of Authors:	Peter Kluit, Ph.D. Jochen Kaminsky, Dr other authors not listed here
Abstract:	<p>A Time Projection Chamber (TPC) module with 32 GridPix chips was constructed and the performance was measured using data taken in a testbeam at DESY in 2021. The GridPix chips each consist of a Timepix3 ASIC (TPX3) with an integrated amplification grid and have a high efficiency to detect single ionisation electrons. In the testbeam setup, the module was placed in between two sets of Mimosas26 silicon detector planes that provided external high precision tracking and the whole detector setup was slid into the PCMAG magnet at DESY. The analysed data were taken at electron beam momenta of 5 and 6 GeV/c and at magnetic fields of 0 and 1 Tesla(T).</p> <p>The result for the transverse diffusion coefficient DT is $287 \mu\text{m}/\sqrt{L}$ at $B = 0$ T and DT is $121 \mu\text{m}/\sqrt{L}$ at $B = 1$ T. The longitudinal diffusion coefficient DL is measured to be $268 \mu\text{m}/\sqrt{L}$ at $B = 0$ T and $252 \mu\text{m}/\sqrt{L}$ at $B = 1$ T. The diffusion measurements have negligible errors.</p> <p>Results for the tracking systematical uncertainties in xy (pixel plane) were measured to be smaller than $13 \mu\text{m}$ with and without magnetic field. The tracking systematical uncertainties in z (drift direction) were smaller than $15 \mu\text{m}$ ($B = 0$ T) and $20 \mu\text{m}$ ($B = 1$ T).</p>
Suggested Reviewers:	<p>Fabio Sauli European Organization for Nuclear Research fabio.sauli@cern.ch World expert</p> <p>Daniela BORTOLETTO European Organization for Nuclear Research daniela.bortoletto@cern.ch</p> <p>Maksym Titov maxim.titov@cea.fr Gaseous detector expert</p>
Opposed Reviewers:	

Towards a Pixel TPC part I: construction and test of a 32 chip GridPix detector

M. van Beuzekom^a, Y. Bilevych^b, K. Desch^b, S. van Doesburg^a,
H. van der Graaf^a, F. Hartjes^a, J. Kaminski^b, P.M. Kluit^a,
N. van der Kolk^a, C. Ligtenberg^a, G. Raven^a, J. Timmermans^a

^a*Nikhef, Science Park 105, 1098 XG Amsterdam, The Netherlands*

^b*Physikalisches Institut, University of Bonn, Nussallee 12, 53115 Bonn, Germany*

Abstract

A Time Projection Chamber (TPC) module with 32 GridPix chips was constructed and the performance was measured using data taken in a testbeam at DESY in 2021. The GridPix chips each consist of a Timepix3 ASIC (TPX3) with an integrated amplification grid and have a high efficiency to detect single ionisation electrons. In the testbeam setup, the module was placed in between two sets of Mimosas26 silicon detector planes that provided external high precision tracking and the whole detector setup was slid into the PCMAG magnet at DESY. The analysed data were taken at electron beam momenta of 5 and 6 GeV/c and at magnetic fields of 0 and 1 Tesla(T).

The result for the transverse diffusion coefficient D_T is $287 \mu\text{m}/\sqrt{cm}$ at $B = 0$ T and D_T is $121 \mu\text{m}/\sqrt{cm}$ at $B = 1$ T. The longitudinal diffusion coefficient D_L is measured to be $268 \mu\text{m}/\sqrt{cm}$ at $B = 0$ T and $252 \mu\text{m}/\sqrt{cm}$ at $B = 1$ T. The diffusion measurements have negligible errors. Results for the tracking systematical uncertainties in xy (pixel plane) were measured to be smaller than $13 \mu\text{m}$ with and without magnetic field. The tracking systematical uncertainties in z (drift direction) were smaller than $15 \mu\text{m}$ ($B = 0$ T) and $20 \mu\text{m}$ ($B = 1$ T).

Keywords:

Micromegas, gaseous pixel detector, micro-pattern gaseous detector,

*Corresponding author. Telephone: +31 20 592 2000
Email address: s01@nikhef.nl (P.M. Kluit)

1. Introduction

Earlier publications on a single chip [1] and four chip (quad) GridPix detectors [2] showed the potential of the GridPix technology and the large range of applications for these devices [3]. In particular, it was demonstrated that single ionisation electrons can be detected with high efficiency and great precision, allowing excellent 3D track position measurements and particle identification based on the number of electrons and clusters.

As a next step towards a Pixel Time Projection Chamber for a future collider experiment [4], [5], a module consisting of 32 GridPix chips based on the TPX3 chip was constructed.

A GridPix detector consists of a CMOS pixel TPX3 chip [6] with integrated amplification grid added by photolithographic - Micro-electromechanical Systems (MEMS) - postprocessing techniques. The TPX3 chip can be operated with a low threshold of $515 e^-$, and has a low equivalent noise charge of about $70 e^-$. The GridPix single chip and quad detectors have a very fine granularity of $55 \times 55 \mu m^2$ and a high efficiency to detect single ionisation electrons.

Based on the experience gained with these detectors a 32 GridPix detector module - consisting of 8 quads - was built. A drift box defining the electric field and gas envelop was constructed. A readout system for up to 128 chips with 4 multiplexers readout by one Speedy Pixel Detector Readout SPIDR board [7] [8] was designed. After a series of tests using the laser setup [9] and cosmics in the laboratory at Nikhef, the detector was taken to DESY for a two week testbeam campaign.

At DESY the 32 chip detector was placed in between two sets of Mimosa26 silicon detector planes and mounted on a movable stage. The whole detector setup was slid into the centre of the PCMAG magnet at DESY. A beam trigger was provided by scintillator counters. The data reported here were taken at different stage positions and electron beam momenta of 5 and 6 GeV/c and at magnetic fields of 0 and 1 T. The performance of the 32 GridPix detector module was measured using these data sets.

In this paper part I of the results will be presented with the main focus on the detector spatial resolution and tracking performance. A second follow up paper will discuss the dE/dx (or dN/dx) and other results.

2. The 32 GridPix detector module

A 32 GridPix detector module was built using the quad module [2] as a basic building block. The quad module consists of four GridPix chips and is optimised for a high fraction of sensitive area of 68.9%. The external dimensions are 39.60 x 28.38 mm. The four chips which are mounted on a cooled base plate (COCA), are connected with wire bonds to a common central 6 mm wide PCB. A 10 mm wide guard electrode is placed over the wire bonds 1.1 mm above the aluminium grids, in order to prevent field distortions of the electric drift field. The guard is the main inactive area, and its dimensions are set by the space required for the wire bonds. On the back side of the quad module, the PCB is connected to a low voltage regulator. The aluminium grids of the GridPixes are connected by 80 μm insulated copper wires to a high voltage (HV) filtering board. The quad module consumes about 8W of power of which 2W is used in the LV regulator.

Eight quad modules were embedded in a box, resulting in a GridPix detector module with a total of 32 chips. A schematic 3-dimensional drawing of the detector is shown in Figure 1. A schematic drawing of the quads in the module is shown in Figure 2, where also the beam direction is indicated.

The internal dimensions of the box are 79 mm along the x -axis, 192 mm along the y -axis, and 53 mm along the z -axis (drift direction), and it has a maximum drift length (distance between cathode and readout anode) of 40 mm. The drift field is shaped by a series of parallel CuBe field wires of 75 μm diameter with a wire pitch of 2 mm and guard strips are located on all of the four sides of the active area. In addition, six guard wires - shown with dashed lines in Figure 2 - are suspended over the boundaries of the chips, where no guard is present, to minimise distortions of the electric drift field. The wires are located at a distance of 1.15 mm from the grid planes, and their potential is set to the drift potential at this drift distance. The box has two Kapton 50 μm windows to allow the beam to pass with minimal multiple scattering.

The gas volume of 780 ml is continuously flushed at a rate of ~ 50 ml/min (about 4 volumes/hour) with premixed T2K TPC gas. This gas is a mixture consisting of 95% Ar, 3% CF_4 , and 2% iC_4H_{10} suitable for large TPCs because of the low transverse diffusion in a magnetic field and the high drift velocity.

The data acquisition system of the quad module was adopted to allow for reading out multiple quads. A multiplexer card was developed that handles four quads or 16 chips and combines the TPX3 data into one data stream.

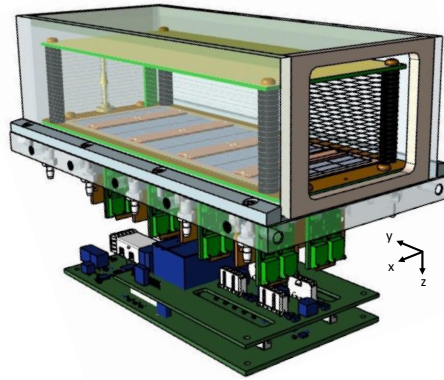


Figure 1: Schematic 3-dimensional render of the 8-quad module detector for illustration purposes.

For the 32 GrixPix module two multiplexers are connected to a SPIDR board that controls the chips and readout process. The readout speed per chip is 160 Mbps and for the multiplexer 2.56 Gbps this corresponds to a maximum rate of 21MHits/s. For each pixel the precise Time of Arrival (ToA) using a 640 MHz TDC and the time over threshold (ToT) are measured.

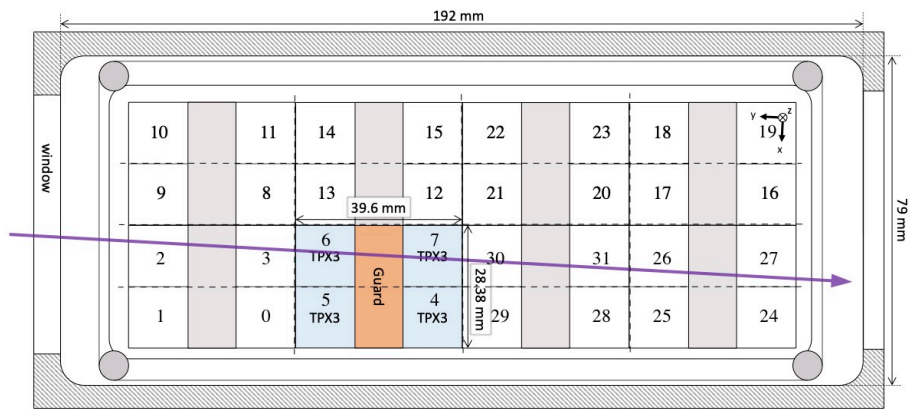


Figure 2: Schematic drawing of the 8-quad module detector with one example quad as viewed from the top of the quads. The chips are numbered and the beam direction is shown in purple.

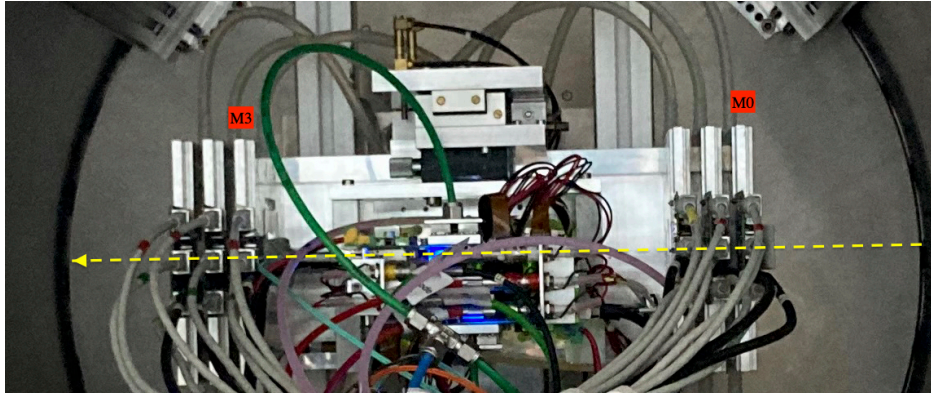


Figure 3: Photo of the detector setup at the centre of the PCMAG magnet. The Mimosa26 planes M0 and M3 are indicated in red as well as the beam direction (yellow). Centrally, the stage positions the TPC module with respect to the beam and the Mimosa26 planes.

3. Experimental setup

In preparation of the two weeks DESY testbeam campaign, a support frame was designed to move the 32 chip GridPix detector module in the plane perpendicular to the beam by a remotely controlled stage such that the whole detector volume could be probed. The module was mounted upside down with respect to figure 1 to allow access to the electronics from above. The support frame also held three Mimosa26 silicon detector planes [10] - with an active area of (21.2 mm x 10.6 mm) - placed in front of the detector and three Mimosa26 planes behind the detector. At DESY the (Mimosa26) silicon detector planes were provided by the testbeam coordinators. The whole detector setup was slid towards the centre of the PCMAG magnet at the DESY II testbeam facility [10]. A beam trigger was provided by a double scintillator counter coincidence. The data were taken at different stage positions to cover the whole sensitive TPC volume. Runs with electron beam momenta of 5 and 6 GeV/c and at magnetic fields of 0 and 1 T were analysed.

A photograph of the detector setup in the PCMAG magnet is shown in Figure 3.

The experimental and environmental parameters such as temperature, pressure, gas flow, oxygen content were measured and logged by a Windows operated slow control system. The experimental parameters are summarised in Table 1. The chips were cooled by circulating Glycol through the cooling

channels in the module carrier plate. The cooling blocks of the multiplexers were further cooled by blowing pressurised air on them.

Table 1: Overview of the experimental parameters. The ranges indicate the variation over the data taking period

Number of analysed runs at B=0 (1) T	6 (8)
Run duration	10-90 minutes
Number of triggers per run	3-100 k
E_{drift}	280 V/cm
V_{grid}	340V
Threshold	550 e ⁻
Gas temperature	303.3-306.6 K
Pressure	1011 – 1023 mbar
Oxygen concentration	240 - 620 ppm
Water vapour concentration	2000 - 7000 ppm

The data was produced in four main data streams: one stream produced by the Mimosa26 Telescope, two data streams by the two Timepix multiplexers and one trigger stream. The double scintillator coincidence provided a trigger signal to the Trigger Logic Unit (TLU) [11] that sends a signal to the telescope readout and the trigger SPIDR. The data acquisition system of the Telescope and trigger SPIDR injected a time stamp into their respective data streams. Hits from the Mimosa26 planes were collected with a sliding window of $-115 \mu\text{s}$ to $230 \mu\text{s}$ of the trigger. The data acquisition of the multiplexer and the trigger SPIDR were synchronised at the start of the run. By comparing the time stamps in these streams, Telescope tracks and TPC tracks could be matched. Unfortunately, the SPIDR trigger had - due to a cabling mistake at the output of the TLU - a common 25ns flat time jitter.

After a short data taking period one of the chips (nr 11) developed a short circuit and the HV on the grid of the chip was disconnected. After the testbeam data taking period the module was repaired in the clean room in Bonn.

4. Analysis

4.1. Telescope Track reconstruction procedure

The data of the Telescope is decoded and analysed using the Corryvreckan software package [12]. The track model used for fitting was the General

Broken Lines (GBL) software [14]. The code was extended and optimised to fit curved broken lines for the data with magnetic field. The telescope planes were iteratively aligned using the standard alignment software provided by the package. The single point Mimosas26 resolution is $4 \mu\text{m}$ in x and $6 \mu\text{m}$ in z (drift direction) [10].

Telescope tracks were selected with at least 5 out of the 6 planes on the track and a total χ^2 of better than 25 per degree of freedom. The uncertainties on the Telescope track prediction in the middle of the GridPix detector module are dominated by multiple scattering. The amount of multiple scattering was estimated by comparing the predictions from the two telescope arms for $6 \text{ GeV}/c$ tracks at $B = 0 \text{ T}$. The expected uncertainty in x and z is $26 \mu\text{m}$ on average.

4.2. TPC Track reconstruction procedure

GridPix hits are selected requiring a minimum time over threshold ToT of $0.15 \mu\text{s}$. The drift time is defined as the measured time of arrival minus the trigger time recorded in the trigger SPIDR data stream minus a fixed t_0 (the drift time at zero drift). The drift time was corrected for time walk [2] using the measured time over threshold (ToT in units of μs) and the formula (1):

$$\delta t = \frac{18.6(ns \mu s)}{\text{ToT} + 0.1577(\mu s)}. \quad (1)$$

Furthermore, small time shift corrections - with an odd-even and a 16×2 pixels structure - coming from the TPX3 clock distribution were extracted from the data and applied.

The z drift coordinate was calculated as the product of the drift time and the drift velocity. This implies that $z_{\text{drift}} = -z$ as defined in figure 1. GridPix hits outside an acceptance window of 30 mm wide in x and 15 mm wide in z were not used in the track finding and reconstruction. Based on a Hough transform an estimate of the TPC track position and angles in the middle of the module (at $y = 1436$ pixels) was obtained. This estimate was used to collect the hits around the TPC track and fit the track parameters. For this fit a straight line ($B = 0 \text{ T}$) or a quadratic track $B = 1 \text{ T}$ model was used. In the fit, the expected uncertainties per hit σ_x and σ_z were used. The fit was iterated three times to perform outlier removal at respectively 10, 5 and 2.5 sigma level. A TPC track was required to have a least 100 hits in each multiplexer. At least 25% of the total number of hits should be on

Table 2: Table with track/event selection cuts

$$\begin{aligned}
 & \text{Track/Event Selection} \\
 & |x_{\text{TPC}} - x_{\text{Telescope}}| < 0.3 \text{ mm} \\
 & |z_{\text{TPC}} - z_{\text{Telescope}}| < 2 \text{ mm} \\
 & |dx/dy_{\text{TPC}} - dx/dy_{\text{Telescope}}| < 4 \text{ mrad} \\
 & |dz/dy_{\text{TPC}} - dz/dy_{\text{Telescope}}| < 2 \text{ mrad}
 \end{aligned}$$

track and the χ^2 per degree of freedom had to be less than 3 in xy and zy. All track parameters were expressed at a plane in the middle of the TPC.

The calibration and alignment of the detector was done using high quality tracks for which the track selections are summarised in table 2.

The drift velocity was calibrated per run by fitting a linear function to the z (predicted from the Telescope track at the measured TPC hit position) versus the measured drift time in the TPC. For the B = 0 T runs it varies between 61.6 and 63.0 $\mu\text{m}/\text{ns}$. For the B = 1 T runs it is between 57.2 and 59.1 $\mu\text{m}/\text{ns}$. The variation comes mainly from the changes in the relative humidity of the gas volume due to small leaks.

The individual TPX3 chips were iteratively aligned fitting a shift in x (z drift) and two slopes $dx(z \text{ drift})/d \text{ row}(\text{column})$. The alignment was done per run, because the detector was moved in x and/or z for each run. The fitted slopes were also corrected for small shifts and rotations (3D) in the nominal chip position.

An example event run 6916 without B field with a TPC and a telescope track is shown in figure 4. The TPC is located between $y = 0$ and 2872 pixels. Three Mimosas26 planes are located at $y < -1000$ and three at $y > 4000$ pixels.

5. Hit resolutions

In order to study the single electron resolution for the data with and without magnetic field, additional selections on the Telescope and TPC tracks were applied. Due to the trigger time jitter of 25 ns (corresponding to 1.5 mm drift), the prediction of the telescope track in z must be used as the reference for z. Secondly, the z hits of the TPC track were fitted to correct for the common time shift and the z residuals were calculated with respect to the fitted TPC track. In the xy plane the residuals of TPC hits with respect to the telescope track were used to extract the single electron resolution in

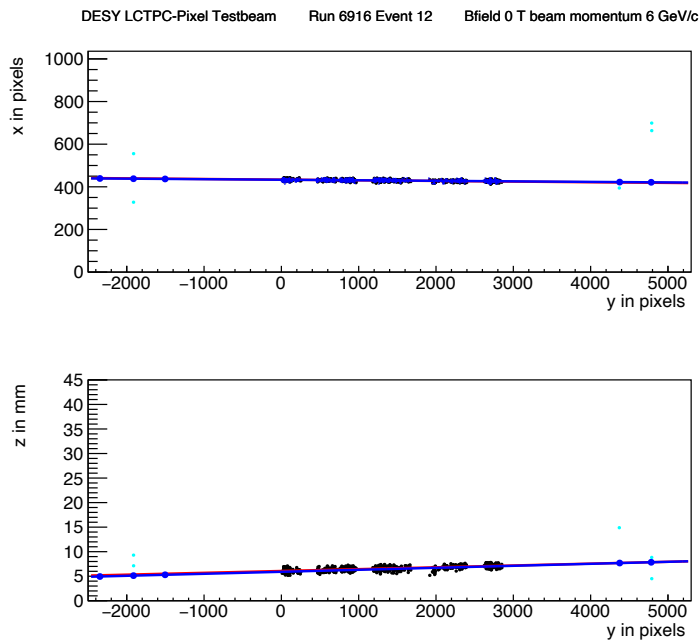


Figure 4: An event display for run 6916 without B field, with in total 1293 TPC hits (black dots) in the precision plane (x,y) and driftplane (z drift,y). The fitted TPC track (red line) with 1130 hits on track and the telescope track (blue line) with 5 Mimosas26 planes (blue hits) on track are shown. In green the off track Mimosas26 hits are shown.

xy. For the resolution studies runs at three different z stage positions of the TPC were selected where the beam gave hits in the central chips. The data of 14 central chips (9, 12, 21, 20, 17, 16, 2, 3, 6, 7, 30, 31, 26 and 27) was used. Two chips (8 and 13) were left out because of the E field deformations caused by the short circuit in chip 11.

5.1. Hit resolutions in the pixel plane

The resolution of the hits in the pixel plane (xy) was measured as a function of the predicted drift position (z_{drift}). Only hits are used crossing the fiducial region defined by the central core of the beam and staying 20 pixels away from the chip edges. The resolution for the detection of ionisation electrons σ_x is given by:

$$\sigma_x^2 = \frac{d_{\text{pixel}}^2}{12} + d_{\text{track}}^2 + D_T^2(z_{\text{drift}} - z_0), \quad (2)$$

where d_{pixel} is the pixel pitch size, d_{track} the uncertainty from the track prediction, z_0 is the position of the grid, and D_T is the transverse diffusion coefficient. The resolution at zero drift distance $d_{\text{pixel}}/\sqrt{12}$ was fixed to 15.9 μm and d_{track} to 30 μm for $B = 0$ T and 42 μm for $B = 1$ T data. The uncertainty of the track prediction was measured and is larger than the Mimoso plane resolution because of multiple scattering in the sensor and in the entrance and exit windows.

The expression (2) - leaving z_0 and D_T as free parameters - is fitted to the $B = 0$ T data shown in Figure 5. The fit gives a transverse diffusion coefficient D_T of 287 $\mu\text{m}/\sqrt{\text{cm}}$ with negligible statistical uncertainty. The measured value is in agreement with the value of 287 $\mu\text{m}/\sqrt{\text{cm}} \pm 4\%$ predicted by the gas simulation software Magboltz 11.9 [15]. The values of the diffusion coefficients depend on the humidity that was not precisely measured during the testbeam. The humidity strongly affects the drift velocity. Therefore the drift velocity prediction from Magboltz was used to determine the water content per run and predictions for the diffusion coefficients could be obtained.

A fit to the $B = 1$ T data, also shown in Figure 5, gives a transverse diffusion coefficient D_T of 121 $\mu\text{m}/\sqrt{\text{cm}}$ with negligible statistical uncertainty. The measured value is in agreement with the value of 119 $\mu\text{m}/\sqrt{\text{cm}} \pm 2\%$ predicted by Magboltz.

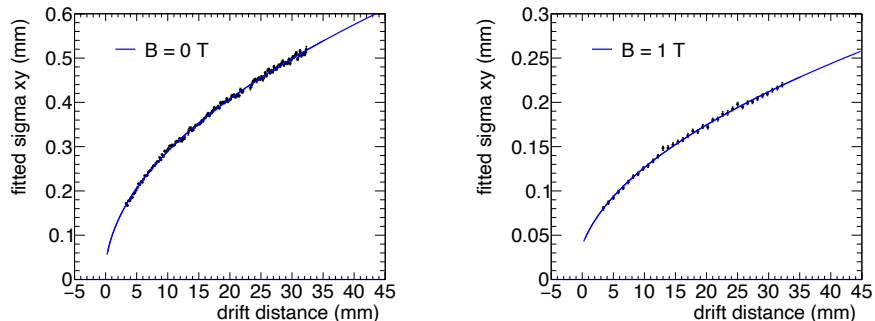


Figure 5: Measured hit resolution in the pixel plane (black points) fitted with the resolution function according to equation (2) (blue line).

5.2. Hit resolution in the drift plane

The resolution for the detection of ionisation electrons σ_z in the drift plane is given by:

$$\sigma_z^2 = \sigma_{z0}^2 + d_{\text{track}}^2 + D_L^2(z_{\text{drift}} - z_0), \quad (3)$$

where σ_{z0} is the resolution at zero drift distance, d_{track} the expected track uncertainty and D_L the longitudinal diffusion constant. Only tracks crossing the fiducial region were accepted and hits with a ToT value above $0.6 \mu\text{s}$ were selected. Because of the time jitter, the fitted TPC track is used for the drift residuals. For z_{drift} the Telescope prediction at the hit was used. The expected uncertainty on the Telescope track prediction is $25 \mu\text{m}$.

The expression (3) - leaving σ_{z0} and D_L as free parameters - is fitted to the $B = 0 \text{ T}$ data shown in Figure 6. The value of z_0 was fixed to the result of the fit in the xy plane. The value of σ_{z0} was measured to be $138 \mu\text{m}$. The longitudinal diffusion coefficient D_L was determined to be $(265 \pm 1) \mu\text{m}/\sqrt{\text{cm}}$, which is higher than the expected value $(236 \pm 3) \mu\text{m}/\sqrt{\text{cm}}$ from a Magboltz calculation [15].

A fit to the $B = 1 \text{ T}$ data shown in Figure 6 gives a longitudinal diffusion coefficient D_L of $(250 \pm 2) \mu\text{m}/\sqrt{\text{cm}}$. The measured value is in agreement with the value of $(245 \pm 4) \mu\text{m}/\sqrt{\text{cm}}$ predicted by Magboltz. The fitted value of σ_{z0} was $133 \mu\text{m}$.

5.3. Deformations in the pixel and drift plane

It is important to measure possible deformations in the pixel (xy) and drift (z) plane to quantify the tracking precision. For the construction of

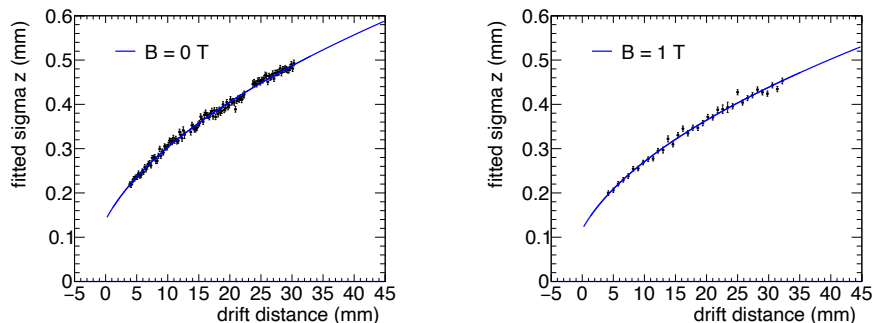


Figure 6: Resolution in the drift plane for hits with a ToT above $0.60 \mu\text{s}$. The data are fitted with the expression of equation (3).

a large Pixel TPC, deformations in the pixel plane deformation should be controlled to better than typically $20 \mu\text{m}$ because these affect the momentum resolution. The mean residuals in the pixel and drift planes are shown in Figure 7 for the $B = 0 \text{ T}$ data set using a large set of runs to cover the whole module. The residuals were calculated with respect to the Telescope track prediction. Because of limited statistics bins were grouped into 8×16 pixels. Bins with less than 100 hits are left out and residuals larger (smaller) than $\pm 100 \mu\text{m}$ are shown in red (blue).

A few critical areas can be observed in figure 7: the region around chip 11 is affected (chips 14, 8 and 13), because the grid of chip 11 was disconnected. Deformations are present at the four corners of the drift box (chips 1, 10, 19 and 24) and close to the upper corner edge (chip 16) of the drift box. These come from inhomogenities in the drift field near the supporting pillars, the field wires are too close to the chip to provide a constant electric field. It was concluded that for the deformation results the hits of these nine chips have to be removed. The track fit was redone leaving these hits out of the fit, such that they could not bias and affect the results.

In order to reduce the statistical fluctuations and quantify the tracking precision, the module was regrouped in four 256×256 pixel planes put side by side on the horizontal axis, as shown in figure 8. Bins have a size of 16×16 pixels and bins with less than 1000 entries are not shown. A bias in the mean residual at the edge of the chips is expected to be present for an ideal detector because of the finite coverage and the diffusion in the drift process. Due to the presence of the dike pixels at the edge of the chip became covered

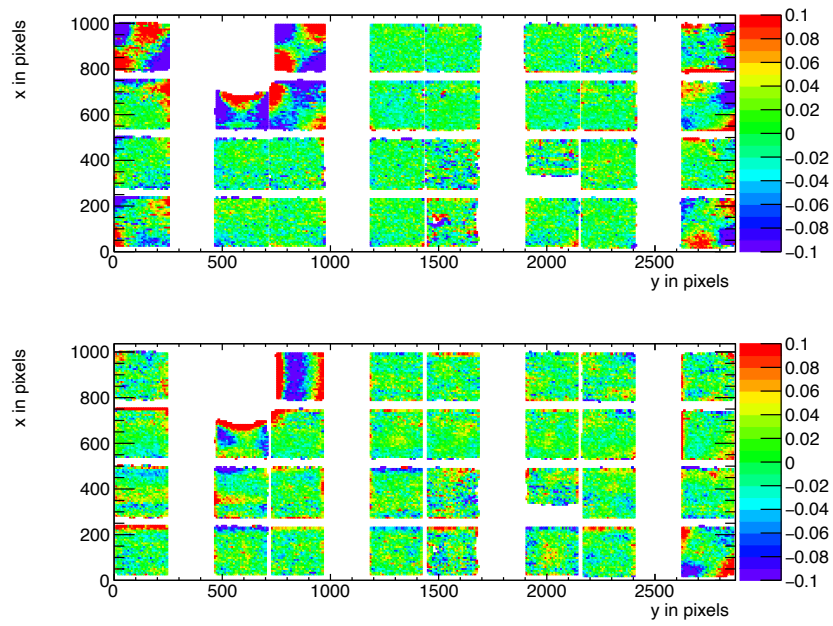


Figure 7: Mean residuals (in mm) in the pixel (top) and drift (bottom) plane for $B = 0$ T data at the expected hit position.

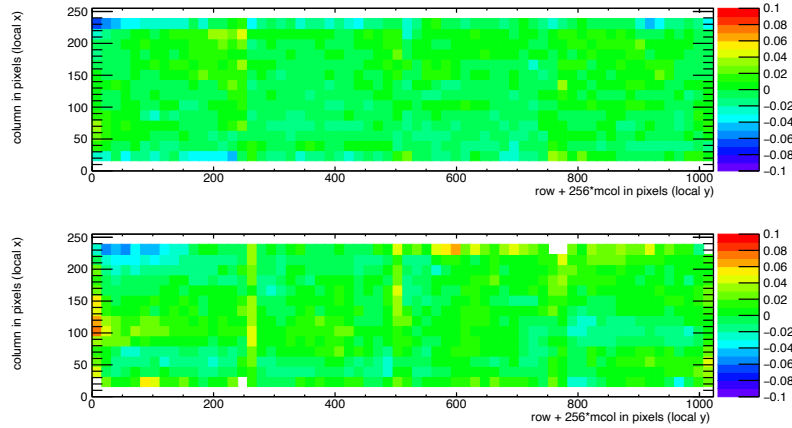


Figure 8: Mean residuals (in mm) in the pixel (top) and drift plane (bottom) for $B = 0$ T data at the regrouped expected hit position.

and inefficient. Therefore the region near the edge of 5 pixels was removed. For the drift coordinate a region of 10 pixels was removed. The total number of measurements (bins) in xy is 895 and in z 892. One can observe that in the module plane no clear systematic deviations are present and conclude that the guard wire voltages were on average well tuned. Note that in the quad module we had no guard wires and deformation corrections had to be applied [2]. The r.m.s. of the distribution of the measured mean residual over the surface in the pixel plane is $11 \mu\text{m}$ and in the drift plane $15 \mu\text{m}$. Similarly, regrouping the module in four planes of 256×256 pixels putting them on top of each other vertically, yielded a r.m.s. in the pixel plane of $13 \mu\text{m}$ and $13 \mu\text{m}$ in the drift coordinate. The expected statistical error in xy is $4 \mu\text{m}$ and in z $5 \mu\text{m}$.

In the $B = 1$ T data set, the electrons will drift mainly along the magnetic field lines. Deformations are in that case due to e.g. the non-alignment of the electric and magnetic field, giving $E \times B$ effects. Unfortunately, the statistics of the Telescope tracks that have a matched TPC track was insufficient and did not cover the full TPC module plane. Therefore the larger statistics of matched and unmatched TPC tracks was used. TPC tracks were required to pass angular selection cuts (dx/dy between -40 and -20 mrad and dz/dy between 0 and 14 mrad) and a momentum cut ($p > 2 \text{ GeV}/c$ and $q < 0$).

The mean residuals in the pixel and drift planes are shown in figure 9 for the $B = 1$ T data set using a large set of runs to cover the whole module. The

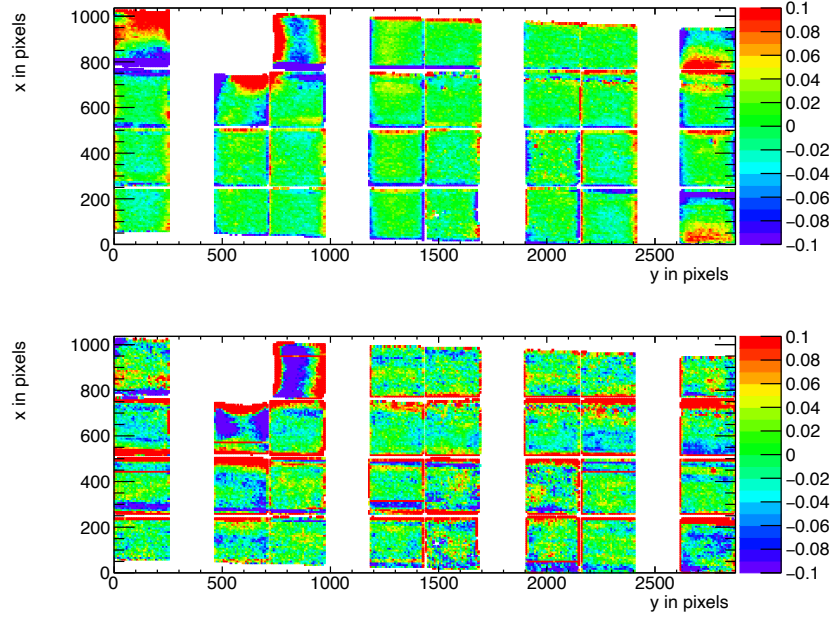


Figure 9: Mean residuals in the pixel and drift plane for $B = 1$ T data at the expected hit position.

residuals were calculated with respect to the TPC track prediction. Because of limited statistics bins were grouped into 8×16 pixels. Bins with less than 100 hits are left out and residuals larger (smaller) than $\pm 100 \mu\text{m}$ are shown in red (blue).

In figure 9 the critical areas discussed above - around chip 11, the four corner chips and chip 16 in the upper corner edge - can be clearly observed. For the deformation results the hits of these nine chips have to be removed. The TPC track fit was redone leaving these hits out of the fit, thus that they could not bias and affect the results. The TPC plane is well covered, although one can observe that due to the angle of the beam in the xy plane the chips in the upper right and lower left corners are not fully covered.

In order to reduce the statistical fluctuations and quantify the tracking precision, the module was regrouped in four 256×256 pixel planes put side by side on the horizontal axis, as shown in figure 10. Bins have a size of 16×16 pixels and bins with less than 1000 entries are not shown. Similar to the no-field deformations studies, acceptance cuts had to be applied. The region near the edge of 16 pixels (columns) was removed. For the drift coordinate

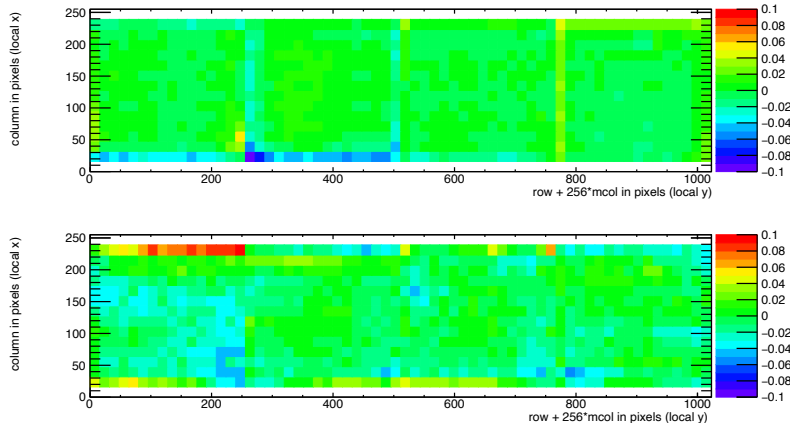


Figure 10: Mean residuals in the pixel and drift plane for $B=1\text{T}$ data at the regrouped expected hit position.

in addition a region of 10 pixels (rows) was removed. The total number of measurements (bins) in xy is 896 and in z 896. One can observe that in the module plane no clear systematic deviations are present. The r.m.s. of the distribution of the measured mean residual over the surface in the pixel plane is $13\ \mu\text{m}$ and in the drift plane $19\ \mu\text{m}$. Similarly, regrouping the module in four planes of 256×256 pixels side by side vertically, yielded a r.m.s. in the pixel plane of $11\ \mu\text{m}$ and $20\ \mu\text{m}$ in the drift coordinate. The expected statistical error in xy is $2\ \mu\text{m}$ and in z $3\ \mu\text{m}$.

5.4. Tracking resolution

A selected TPC track in the $B = 0\ \text{T}$ data has on average 1000 hits. The tracking precision in the middle of the TPC was derived on a track-by-track basis and found to be on average $9\ \mu\text{m}$ in the precision plane and $13\ \mu\text{m}$ in z . The angular resolution in dx/dy was on average $0.19\ \text{mrad}$ and for dz/dy $0.25\ \text{mrad}$. It is clear that the position resolution in the TPC in the precision and drift coordinates is impressive for a track length of (only) $158\ \text{mm}$. The values are smaller than the uncertainty on the track prediction from the silicon telescope of $26\ \mu\text{m}$ on average that is dominated by multiple scattering.

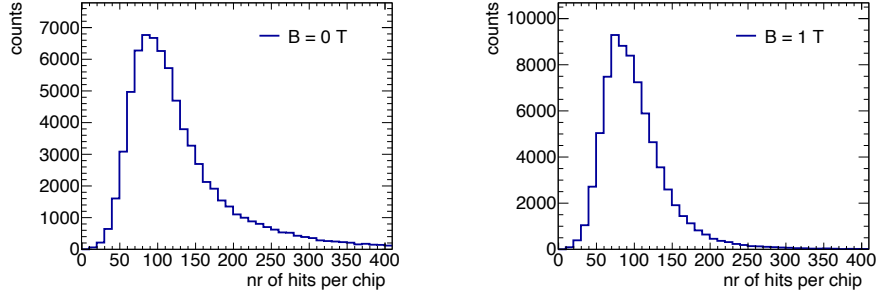


Figure 11: Distribution of the number of track hits per per chip for $B = 0$ T (left) $B = 1$ T data.

6. Single electron efficiency

The distribution of the number of TPC track hits per chip - without requiring a matched Telescope track - are shown in figure 11 for the data without magnetic field and for the $B = 1$ T data. The $B = 0$ T data analysis selects the central chips 2,6,7,9,16,17,26 and 27. The $B = 1$ T data analysis selects the same chips plus chips 12,13,20 and 21.

The mean number of hits is measured to be 124 and 89 in the $B = 0$ T and 1 T data sets respectively. The most probable values are respectively 87 and 64. Note that the $B = 0$ T data have a much larger Landau-like tail than the 1 T data. Also the fluctuations in the core of the distribution are larger. The mean time over threshold is $0.68 \mu\text{s}$ for the $B = 0$ T and $0.86 \mu\text{s}$ at a $B = 1$ T data. This means that the deposited charge per pixel is smaller for the 0 T data. The most probable value for the total deposited charge is similar for both data sets. A possible explanation for this behavior is that because of the reduced transverse diffusion in the $B = 1$ T data, the possiblity of two primary electrons ending up in a single grid hole is higher. The mean number of hits is in agreement with the predictions of [13] 106 electron-ion pairs for a $6 \text{ GeV}/c$ electron at $B = 0$ T, crossing 236 pixels or 12.98 mm and a detector running at 85% single electron efficiency.

7. Conclusion and outlook

A Time Projection Chamber module with 32 GridPix chips was constructed and the performance was measured using data taken in a testbeam

at DESY in 2021. The analysed data were taken at electron beam momenta of 5 and 6 GeV/c and at magnetic fields of 0 and 1 T.

The result for the transverse diffusion coefficient D_T is $287 \mu\text{m}/\sqrt{cm}$ at $B = 0$ T and D_T is $121 \mu\text{m}/\sqrt{cm}$ at $B = 1$ T. The longitudinal diffusion coefficient D_L is measured to be $268 \mu\text{m}/\sqrt{cm}$ at $B = 0$ T and $252 \mu\text{m}/\sqrt{cm}$ at $B = 1$ T. Results for the tracking systematical uncertainties in xy were measured to be smaller than $13 \mu\text{m}$ with and without magnetic field. The tracking systematical uncertainties in z were smaller than $15 \mu\text{m}$ ($B = 0$ T) and $20 \mu\text{m}$ ($B = 1$ T).

The mean number of hits is in agreement with the predictions of [13] and a detector running at 85% single electron efficiency.

Not all data were analysed and users are welcome to study them using the data sets on available on the Grid.

The GridPix detector will be further tested and developed in view of a TPC that will be installed in a heavy ion experiment at the EIC or other future colliders. A follow up paper is in preparation on the measured dE/dx or dN/dx resolution and other performance topics.

Acknowledgements

This research was funded by the Netherlands Organisation for Scientific Research NWO. The authors want to thank the support of the mechanical and electronics departments at Nikhef and the detector laboratory in Bonn. The measurements leading to these results have been performed at the Test Beam Facility at DESY Hamburg (Germany), a member of the Helmholtz Association (HGF).

References

- [1] C. Ligtenberg, et al., Performance of a GridPix detector based on the Timepix3 chip, Nucl. Instrum. Meth. A 908 (2018) 18–23. arXiv:1808.04565, doi:10.1016/j.nima.2018.08.012.
- [2] C. Ligtenberg, et al., Performance of the GridPix detector quad, Nucl. Instrum. Meth. A 956 (2020) 163331. arXiv:2001.01540, doi:10.1016/j.nima.2019.163331.
- [3] J. Kaminski, Y. Bilevych, K. Desch, C. Krieger, M. Lupberger, GridPix detectors - introduction and applications, Nucl. Instrum. Meth. A845 (2017) 233–235. doi:10.1016/j.nima.2016.05.134.

- [4] C. Ligtenberg, A GridPix TPC readout for the ILD experiment at the future International Linear Collider, Ph.D. thesis, Free University of Amsterdam (2021).
URL https://www.nikhef.nl/pub/services/biblio/theses_pdf/thesis_C_Ligtenberg.pdf
- [5] M. Lupberger, Y. Bilevych, H. Blank, D. Danilov, K. Desch, A. Hamann, J. Kaminski, W. Ockenfels, J. Tomtschak, S. Zigann-Wack, Toward the Pixel-TPC: Construction and Operation of a Large Area GridPix Detector, *IEEE Trans. Nucl. Sci.* 64 (5) (2017) 1159–1167. doi:10.1109/TNS.2017.2689244.
- [6] T. Poikela, J. Plosila, T. Westerlund, M. Campbell, M. De Gaspari, X. Llopart, V. Gromov, R. Kluit, M. van Beuzekom, F. Zappone, V. Zivkovic, C. Brezina, K. Desch, Y. Fu, A. Kruth, Timepix3: a 65K channel hybrid pixel readout chip with simultaneous ToA/ToT and sparse readout, *JINST* 9 (05) (2014) C05013.
URL <http://stacks.iop.org/1748-0221/9/i=05/a=C05013>
- [7] J. Visser, M. van Beuzekom, H. Boterenbrood, B. van der Heijden, J. I. Muñoz, S. Kulis, B. Munneke, F. Schreuder, SPIDR: a read-out system for Medipix3 & Timepix3, *Journal of Instrumentation* 10 (12) (2015) C12028. doi:10.1088/1748-0221/10/12/C12028.
- [8] B. van der Heijden, J. Visser, M. van Beuzekom, H. Boterenbrood, S. Kulis, B. Munneke, F. Schreuder, SPIDR, a general-purpose readout system for pixel ASICs, *JINST* 12 (02) (2017) C02040. doi:10.1088/1748-0221/12/02/C02040.
- [9] F. Hartjes, A diffraction limited nitrogen laser for detector calibration in high energy physics, Ph.D. thesis, University of Amsterdam (1990).
URL https://www.nikhef.nl/pub/services/biblio/theses_pdf/thesis_F_Hartjes.pdf
- [10] R. Diener et al., The DESY II test beam facility, *Nuclear Instruments and Methods in Physics Research. Section A: Accelerators, Spectrometers, Detectors and Associated Equipment* 922 (2019) 265–286. arXiv:1807.09328, doi:10.1016/j.nima.2018.11.133.
- [11] P. Baesso, D. Cussans, J. Goldstein, , *Journal of Instrumentation* 14 (09) (2019) P09019–P09019. arXiv:2005.00310.
URL <https://doi.org/10.1088/1748-0221/14/09/p09019>

- [12] D. Dannheim, K. Dort, L. Huth, D. Hynds, I. Kremastiotis, J. Kröger, M. Munker, F. Pitters, P. Schütze, S. Spannagel, T. Vanat, M. Williams, , *Journal of Instrumentation* 16 (03) (2021) P03008. doi:10.1088/1748-0221/16/03/p03008. arXiv:2011.12730.
URL <https://doi.org/10.1088/1748-0221/16/03/p03008>
- [13] R. Veenhof, *Garfield - simulation of gaseous detectors, version 9*, Reference W5050 (1984-2010).
URL <https://garfield.web.cern.ch>
- [14] C. Kleinwort, General broken lines as advanced track fitting method, *Nuclear Instruments and Methods in Physics Research Section A: Accelerators, Spectrometers, Detectors and Associated Equipment* 673 (2012) 107–110. doi:10.1016/j.nima.2012.01.024.
- [15] S. F. Biagi, Monte Carlo simulation of electron drift and diffusion in counting gases under the influence of electric and magnetic fields, *Nucl. Instrum. Meth. A* 421 (1-2) (1999) 234–240. doi:10.1016/S0168-9002(98)01233-9.
URL <https://magboltz.web.cern.ch/magboltz>